

## **EFFECT OF FRAGMENT IMPACT ON SHAPED CHARGE FUNCTIONING**

**P.Y. Chanteret**

*ISL, French German Research Institute of Saint-Louis  
BP34, F-68301 Saint-Louis, France*

The effect of a fragment impact on the functioning of a shaped charge is investigated. First, experiments are presented with firing shaped charges that were artificially damaged in order to try to mimic some of the effects occurring in the charge after a fragment impact. Then experiments are described where a powder gun is used for shooting steel spheres at shaped charges. Radiographic observations are presented of the jet formation after some time delay between fragment impact and charge initiation. Typical 3D simulations of shaped charge functioning after fragment impact are presented, which illustrate the perturbations in jet formation. Some results of the influence of fragment impact location on shaped charge residual performance are given.

### **INTRODUCTION**

With the emergence of active defense for protecting tanks, the idea of firing a fragmentation warhead against an incoming antitank rocket or missile was one of the first concepts to be considered. The Russian system ARENA was developed using this concept, with launching defensive fragmentation warheads at incoming rockets and missiles [1]. It is usually admitted that the approaching weapon is defeated once fragments hit the shaped charge. However, it is of importance both for designing such counter warheads and also for performing system analysis, to have a more exact knowledge of the quantitative effects of fragment impact on a shaped charge. Such information about the potential of a damaged shaped charge is particularly required for being able to perform simulations using system analysis software [2,3].

In the following, this problem is experimentally investigated using radiographic observation of jet formation and penetration measurements, with both artificially damaged or fragment impacted shaped charges.

### **ARTIFICIALLY DAMAGED CHARGES**

The problem that is to be studied is that of the effect of a fragment impact on a shaped charge in terms of jet residual performance. One has to take into account the fact that

there may exist both the situation where fragments impact the outer part of the charge but also the case where a fragment impacts on the inside of the liner. In the ARENA system, the fragments trajectories intersect the shaped charge trajectory at a large angle and therefore impact almost only on the outer of the charge. But there also exist defense systems in which the splinters are fired in front of the incoming charge, impacting in the shaped charge cavity at angles that could be lower than  $20^\circ$ .

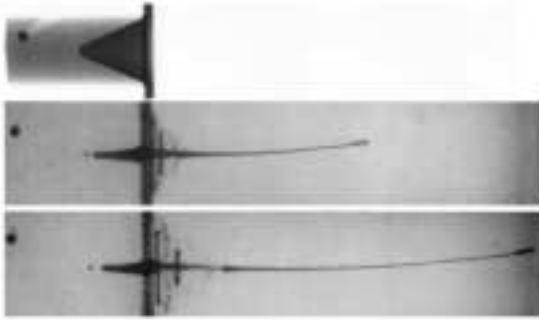


Figure 2: X-ray pictures of the 45 mm conical charge depicted on Fig 1, with a cylindrical hole and a steel sphere in its rear part at  $32 \mu\text{s}$  and  $45 \mu\text{s}$ .

charge plane of symmetry. The hole diameter is equal to 7 mm and its axis makes a  $30^\circ$  angle with the charge axis. A steel sphere is placed in the bottom of the hole with its center being at 10 mm from the charge axis.

Fig. 2 presents three X-ray pictures of the charge at rest and at  $32 \mu\text{s}$  and  $45 \mu\text{s}$  after initiation. This figure shows that a coherent jet is formed, which is only affected by a transverse velocity. It is not surprising to note that such a jet is very similar to what can be observed when a shaped charge is fired with an off-axis initiation [4].

The jet penetration was recorded at a 6 caliber standoff and was estimated to be 30% of that of the undamaged charge. But the charge performance would have probably been higher at lower standoff. From the measurement of lateral jet velocities together with using an analytical shaped charge code, it can be estimated that at 2 calibers standoff, such a jet would have reached 60% of the performance of the undamaged charge.

In the second experiment where the charge depicted on Fig. 3 was fired, it was intended to mimic a much more damaging impact in a charge region closer to the liner. As shown on the picture, the cylindrical hole was drilled in the explosive and through the liner. As in the previous experiment, the hole has a 7 mm diameter and its axis makes a  $30^\circ$  angle with

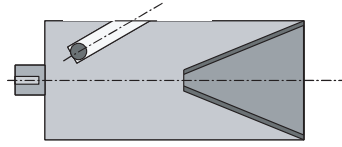


Figure 1:  $45^\circ$  conical charge with a cylindrical hole and a steel sphere in its rear part.

In a first step of the study, shaped charges were fabricated with including artificial modifications intended to mimic – into some extent, a shaped charge that would have been impacted by a fragment. Several such experiments have been performed using  $45^\circ$  conical charges and two examples are presented here which correspond to two very different situations.

Fig. 1 depicts a 45 mm conical shaped charge with a cylindrical hole drilled in the rear region of the explosive, and located in the

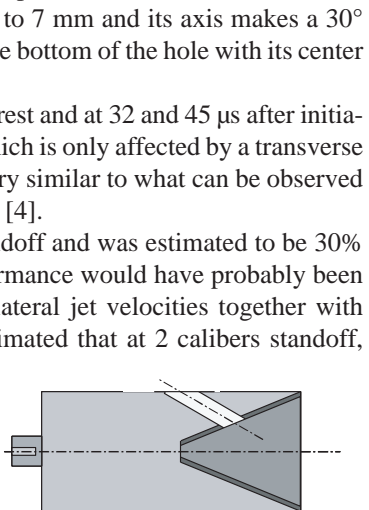


Figure 3:  $45^\circ$  conical charge with a cylindrical hole through explosive and liner.

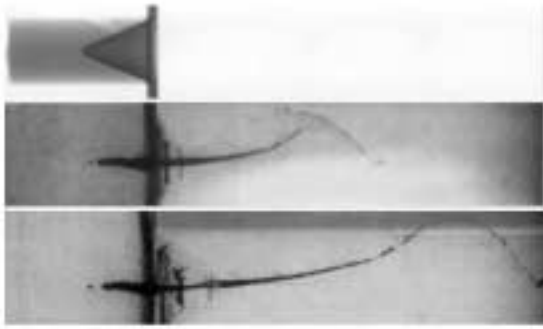


Figure 4: X-ray pictures of the 45 mm conical charge depicted on Fig. 3, with a cylindrical hole in the liner region at 32  $\mu$ s and 45  $\mu$ s.

the charge axis. The cylindrical hole is exiting inside the cone at half the height of the liner.

The radiographic observation of the jet formation obtained with this charge is presented on Fig. 4. One can see that the whole jet is severely disturbed, with transverse jet velocities as high as 1000 m/s.

Looking at these radiographs, it is not surprising that the penetration depth measured in a mild steel target placed at 6 calibers was found to be lower than 10% of the nominal value. Unlike the previous case, decreasing the standoff would probably not increase notably the performance of such a jet.

In the two typical experiments presented here, the effect of a fragment impact was mimicked by drilling a hole in the charge. In real life, a fragment impacting on the explosive at high velocity would create much more damage into the explosive loading than a cylindrical hole, and this is the reason why the experimental program was continued with real firings of fragments at shaped charges.

## **FIRING FRAGMENTS AT SHAPED CHARGES**

In order to get more accurate information about the functioning of impacted charges, the experimental program was then carried on with the idea of performing more realistic experiments. A 15 mm powder gun was used for firing 5 mm diameter steel spheres at velocities ranging from 1100 to 1500 m/s. The gun muzzle was placed at about 3 meters from the shaped charge with a steel sabot catcher plate stopping the plastic sabot. A contact foil was placed on the charge for recording the instant of impact of the sphere on the charge, and the charge was initiated some delay  $\Delta t$  after impact. First some typical radiographic observations of charge functioning will be presented and then penetration depth measurements will be given.

### **Radiographic observations**

The first experiment described was performed with a 45 mm, 60° conical shaped charge, which was impacted inside the liner by a steel sphere traveling at 1200 m/s. The sphere trajectory was included in the charge plane of symmetry, aiming at half the height of the liner and making a 20° angle with the charge axis. The charge was initiated 105  $\mu$ s after the impact of the sphere.

Fig 5 presents three X-ray pictures with the first picture taken 40  $\mu$ s after impact and 65  $\mu$ s before the charge initiation; the two last pictures been taken respectively 11 and 30  $\mu$ s after the initiation. On the two first pictures, one can see that the liner has been perforated by the sphere and in spite of an apparently limited damage, the third X-ray shows a drastically disturbed jet formation. The jet coherency is poor and one can see almost no jet element on the charge axis.

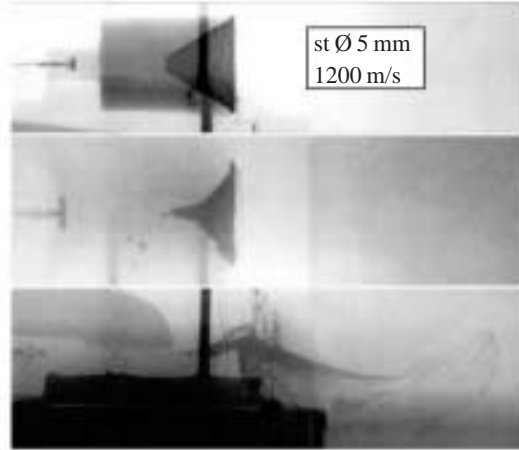


FIGURE 5: 60° conical charge, 45 mm CD impacted by a 5 mm steel sphere at 1200 m/s. Charge initiation at 105  $\mu$ s after impact. X-Rays at -65 $\mu$ s, +11  $\mu$ s and +30  $\mu$ s from initiation.

The second experiment presented was performed using the same impact conditions on a somewhat larger charge. The same 5 mm in diameter steel sphere (0.5 grams) was fired at 1200 m/s, at 20° with the charge axis, and aiming at the liner half height of a 65 mm shaped charge.

As shown on Fig. 6, the charge has a trumpet liner and a light aluminum body on which is placed a contact foil. The steel sphere can easily be seen on the first two radiographs taken before and after impacting on the liner. The charge was initiated 255  $\mu$ s after the impact on the casing, which corresponds to about 140  $\mu$ s after the impact on the liner. The third picture shows the jet 51  $\mu$ s after the charge initiation.

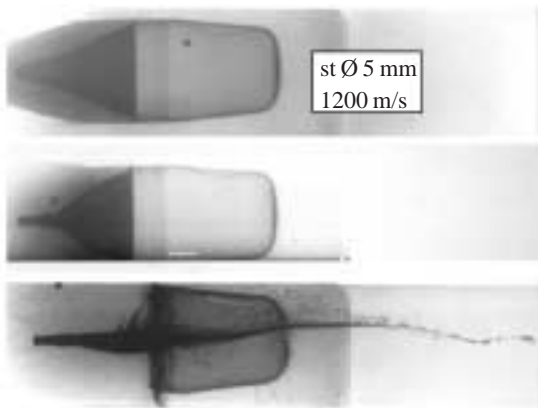


FIGURE 6: 65 mm shaped charge impacted by a 5mm steel sphere at 1200 m/s. Charge initiation at ~140  $\mu$ s after impact on the liner. X-Rays at -150  $\mu$ s, +15  $\mu$ s and +51  $\mu$ s from initiation.

Comparing the jet with the previous experiment depicted on Fig. 5, one can see that the jet is deviated in the same direction, i.e. in the half-plane containing the impacted part of liner. The amount of jet deviation is smaller than in the previous experiment mainly because of the fact that the fragment mass was unchanged for a larger charge. Comparing the two experiments is – to some extent, equivalent to looking at the effects of dividing the fragment mass (or energy) by a factor of three.

## Numerical simulations

Some numerical simulations have been performed using the Eulerian processor of the OTI\*HULL code, in order to see if it would have been possible to reduce the number of experiments. Fig. 7 presents the result of a numerical simulation of the experiment previously described and depicted on Fig. 5. In the calculation, the explosive is initiated on the axis at 15  $\mu$ s after impact. One can see a qualitative agreement in the overall jet deviation, but details in the jet incoherency could not be reproduced although 2 millions cells have been used.

Fig. 8 presents an other example of numerical simulation, in which a 70 mm shaped charge is impacted by a 2 grams steel fragment at 2000 m/s and under 45° incidence. The high explosive was initiated 30  $\mu$ s after fragment impact.

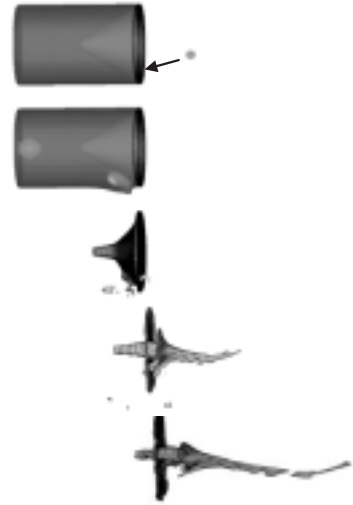


Figure 7: numerical simulation of the experiment on Fig. 5.

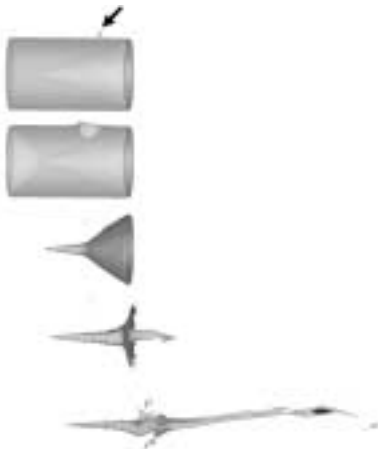


Figure 8:  $\varnothing$  70 mm conical shaped charge impacted by a 2 grams steel fragment at 2 km/s and 45° incidence .

There exist some rather specific difficulties related with the numerical simulation of the detonation of a shaped charge impacted by a fragment. Besides the fact that such 3D simulations require large computing capabilities, one must be able to correctly describe the fragment penetration into the undetonated explosive, and this aspect is difficult to handle as the explosive may be somewhat reacting even if not detonating. The same kind of difficulty concerns the detonation front propagation in the damaged region of the explosive. All these reasons lead to the idea that numerical simulations are of qualitative interest for understanding what happens when no observation are available, but real firings at charges are still required for an estimation of the performance of impacted charges.

## Penetration capability of impacted charges

The shaped charge shown on Fig. 6 was used for a quantitative study of the residual performance of impacted charges. The charge caliber CD is equal to 65 mm; the charge has a trumpet shaped liner and a thin aluminum casing. All the shots were performed

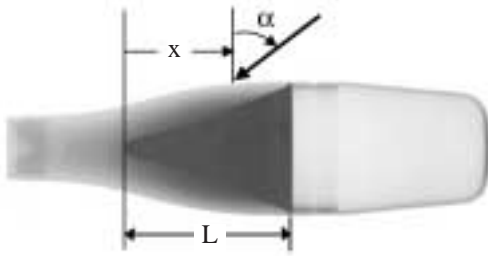


Figure 9: definition of impact conditions.

using the 15 mm powder gun for firing 5 mm steel spheres (0.5 grams) at 1400 m/s. The impact point on the charge and the angle of impact were varied and the residual penetration depth was measured. The angle of impact  $\alpha$  is defined on Fig. 9, where  $\alpha = 0^\circ$  corresponds to a fragment trajectory perpendicular to charge axis and where positive  $\alpha$  values correspond to frontal attack.

Fig. 9 also defines the impact location on the charge casing by its axial distance  $x$  to the liner apex. In the following, the experimental results will be presented as a function of the hit location  $x$  scaled by the liner axial length  $L$ . Therefore negative  $x/L$  values would correspond to fragment impacts located between charge initiation and liner apex, and  $x/L$  values larger than 1 (with  $\alpha$  negative) would correspond to impacts located in the charge nose – therefore impacting inside the cone.

The fragment trajectory was included in the axial plane of symmetry of the charge with the exception of two shots for which the trajectory plane was .25CD off the charge axis.

For all experiments, the fragment impact time was recorded using a contact foil placed at the aimed point on the outer surface of the charge. The charge was then initiated after a 2000  $\mu$ s delay time after the impact. The penetration depth was measured into a mild steel plates stack placed at a 1.5CD standoff distance (charge built-in standoff).

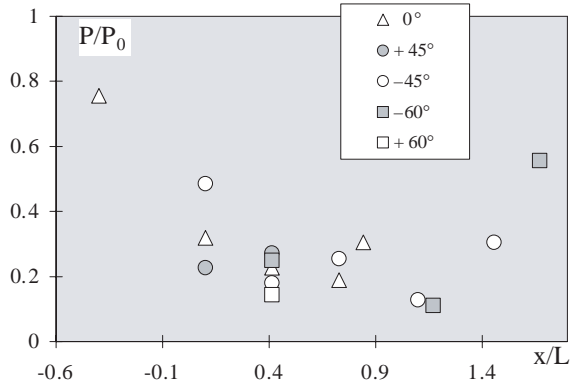


Figure 10: penetration depth of impacted charges as a function of impact location. Charge 65 mm, fragments 0.5 grams, 1400 m/s.

The obtained results are presented on the diagram on Fig. 10 as measured penetration depths  $P$  scaled by the nominal charge performance  $P_0$ , as a function of the scaled impact location  $x/L$ . The different marks on the diagram correspond to the different values for the angle of impact.

It appears that for the impacts that are located close to the liner region, the impacted charges have lost more than 70% of their penetration power as compared to the undamaged charge performance. For the firings where penetration depth was found to be larger than 40% of the nominal performance, it can be seen that they correspond to fragment trajectories which either do not cross the liner (negative or low  $x/L$  values) or which just

touch the basis of the liner (large  $x/L$ ). It must be known that the two shots with a fragment trajectory plane offset from the charge plane of symmetry gave lower penetration depth than for the same  $x/L$  and  $\alpha$  in the plane of symmetry shots: this result could be explained by a higher level of asymmetry in the impacted charge.

The last remark concerning the charge plane of symmetry, together with the fact that measurements were performed into mild steel and with the fact that real  $\alpha$  values would be larger than 2 ms, lead to the deduction that the results presented on Fig. 10 represent an upper limit of the reality. In real situations jets asymmetries could be higher than in our experiments and the decrease in penetration would be larger in armor steel as it is known that the consequences of jet asymmetries increase as target strength increases.

## CONCLUSION

The effects of fragment impact on the functioning of shaped charges have been studied. Radiographic observations and numerical simulations have qualitatively shown how the jet formation can be disturbed by the charge asymmetries produced by the impact of a fragment. Experimental measurements of the residual penetration capability of impacted charges have been collected and these data are available for vulnerability codes and active defense simulations.

## REFERENCES

1. V. Kashin and V. Kharkin, "Active Protection System for Tanks", *Military Parade*, no 5, 32–35, 1996
2. P. Wey and M. Salles, "Simulation and Analysis of Active Defense Systems", *Proceedings of the 17<sup>th</sup> International Symposium on Ballistics*, Midrand, 23–27 March 1998
3. P. Wey, V. Fleck and P.Y. Chanteret, "Analysis of Active Protection Systems: when ATHENA meets ARENA", *Proceedings of the 19<sup>th</sup> International Symposium on Ballistics*, Interlaken, 7–11 May 2001
4. M. Held and P. Nikowitsch, "Inverse Multi-Streak Technique", *Proceedings of the 7<sup>th</sup> Symposium on Detonation*, Annapolis, 16–19 June 1981.

